# 2-(2′-Halophenyl)-α-nitronyl nitroxides[1]

**Shin'ichi Nakatsuji,*,[a] Masako Saiga,[a] Nobuhiko Haga,[a,†] Akira Naito,[a,†] Toshikazu Hirayama,[a] Masahito Nakagawa,[a] Yasukage Oda,[a] Hiroyuki Anzai,*,[a] Kazuya Suzuki,[b] Toshiaki Enoki,[c] Masaki Mito[d] and Kazuyoshi Takeda[d]**

[a] *Department of Material Science and † Department of Life Science, Faculty of Science, Himeji Institute of Technology, Kanaji 1479-1, Kamigori, Hyogo 678-12, Japan*
[b] *Department of Chemistry, Faculty of Engineering, Yokohama National University, 156 Tokiwadai, Hodogaya-ku, Yokohama 240, Japan*
[c] *Department of Chemistry, Faculty of Science, Tokyo Institute of Technology, Meguro-ku, Tokyo 152, Japan*
[d] *Department of Applied Science, Faculty of Engineering, Kyushu University, Fukuoka 812, Japan*

A series of nitronyl nitroxide derivatives of benzene, bearing halogen atoms at the *ortho* position, have been prepared and show a remarkable substituent effect of the *ortho* halogen atoms on their magnetic properties. Among them, the fluorine derivative **1** is found to behave as a ferromagnet with a $T_c$ of around 0.3 K based on ac susceptibility and heat capacity measurements, and its X-ray analysis revealed that the crystals consist of three-dimensional networks of nitroxide radicals bonded through methyl or phenyl groups.

Much attention has recently been focused on the search for new organomagnetic materials and fruitful advances have been achieved in recent years.[2] Since the discovery of the first organic ferromagnet, *i.e.*, the β-phase crystal of *p*-nitrophenyl nitronyl nitroxide,[3] several organic free radicals have been found that show ferromagnetism.[4] The ferromagnetic *p*-nitrophenyl nitronyl nitroxides (β-phase and γ-phase) have been reported to have twisted dihedral angles between the phenyl ring and the plane of the nitronyl nitroxide[5] and similar results were found in some other ferromagnetic radicals. These include 2′,5′-dihydroxy-substituted[6] and 2′-hydroxy-substituted[7] nitronyl nitroxides, which have twisted molecular structures and show ferromagnetic spin–spin interactions in their three-dimensional structures attributed to intra- and intermolecular hydrogen bonds. In order to see the relationship between the molecular, as well as crystal, structures and magnetism in such molecules having a twisted conformation between the π system and the radical moiety, we have prepared nitronyl nitroxide derivatives of benzene by introducing a single atomic substituent, *i.e.*, halogen atom at the *ortho* position (Scheme 1). Gradual distortion between the benzene ring and radical moiety is realized by introducing substituents that cause different three-dimensional crystal structures, due to their steric effect, and thus affect their magnetic properties.

We report in this paper the preparation of four such derivatives **1**–**4**, their magnetic properties and the crystal structures of the fluorine derivative **1** and chlorine derivative **2**.[8]

## MM Calculations and Synthesis of the Radicals 1–4

As an estimation of the distortion between the phenyl ring and the radical moiety of the nitronyl nitroxides **1**–**4**, we first calculated by MM2 calculations the dihedral angles between the plane of the phenyl ring and the O(1)—N(1)—C(1) plane of the radical moiety, which showed a distortion varying with the van der Waals radii of the halogen atoms (Table 1). It was predicted that the dihedral angle for the fluorine derivative **1** should be about 55°, as depicted in Fig. 1.

Following the estimation, we then prepared the nitronyl nitroxide derivatives **1**–**4** from the corresponding *ortho*-substituted benzaldehydes with 2,3-bis(hydroxyamino)-2,3-dimethylbutane sulfate.[9] The anhydrous adducts thus obtained were successively treated with lead dioxide to give

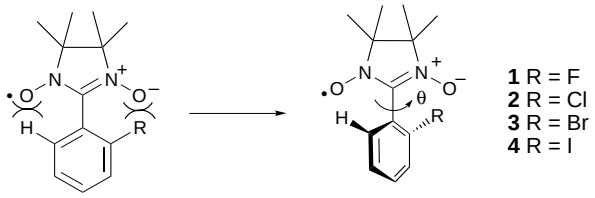


**Scheme 1**

**Table 1** The van der Waals radii of hydrogen and halogen atoms (*r*) and estimated degree of distortion (θ) from MM2 calculation[a]

| Compound | R = H | 1 | 2 | 3 | 4 |
|---|---|---|---|---|---|
| *r*/Å[b] | 1.20 | 1.47 | 1.75 | 1.85 | 1.98 |
| θ/° | 48 (29[c]) | 55 (48[d]) | 66 (60[d]) | 71 | 70 |

[a] Optimized by using MM2 parameters in the CAChe system. [b] In Å, *cf.* A. Bondi, *J. Phys. Chem.*, 1964, **68**, 443. [c] Found by X-ray data; *cf.* W. Wang and S. F. Watkins, *J. Chem. Soc., Chem. Commun.*, 1973, 888. [d] Found by X-ray data; this work.

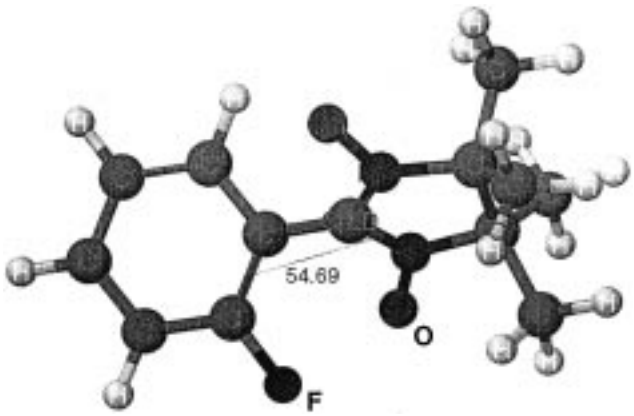


**Fig. 1** Molecular structure of **1** based on MM2 calculations

the desired radicals, which were isolated as relatively stable crystals (for their data, see Experimental section).

## Magnetic Behavior of 1–4

The temperature dependence of the paramagnetic susceptibility of each polycrystalline sample was measured using a SQUID susceptometer (dc susceptibility) in the temperature range 2–300 K. It was found from the plot of the reciprocal susceptibility *vs.* temperature that the fluorine derivative **1** followed the Curie–Weiss law over the whole temperature range, and the Curie and Weiss constants were determined to be 0.375 emu K $mol^{-1}$ and +0.48 K, respectively (Table 2). The positive Weiss constant and the increase in the product $\chi_p T$ with decreasing temperature (lower than *ca.* 20 K) indicate intermolecular ferromagnetic interactions between the spins of radical **1** at low temperature (Fig. 2). The ferromagnetic coupling is further supported by the magnetization curve measurements at low temperature.

The magnetic behavior of **1** was further investigated by ac susceptibility measurements from 0.04 to 4.2 K. As shown in Fig. 3, the phase transition below the Weiss constant (0.48 K) is suggested from the temperature dependence data of $1/\chi_{ac}$ at each applied frequency (20, 40 or 240 Hz). Each peak at around 0.3 K, observed in the temperature dependence data of $\chi_{ac}$, further supports the phase transition as depicted in Fig. 4, in which no apparent difference was observed for different

**Table 2** The Weiss constants of the radicals[a]

| Compound | **1** | **2** | **3** | **4** |
|---|---|---|---|---|
| Θ/K | +0.48 | −2.00 | −3.32 | −3.36 |

[a] The value for the unsubstituted derivative is reported in ref. 15 as Θ/K = −1.4.

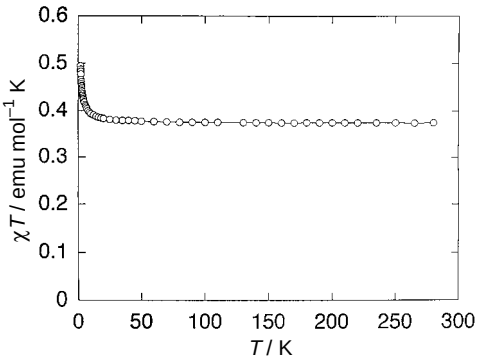


**Fig. 2** Temperature dependence of $\chi T$ for **1**

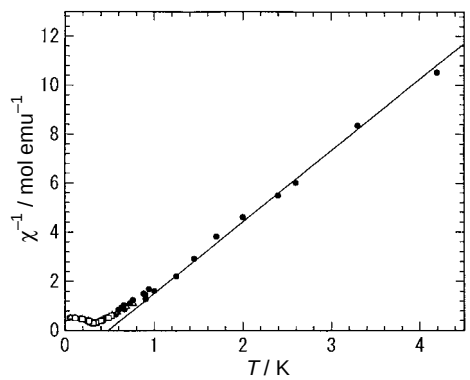


**Fig. 3** Temperature dependence of $1/\chi$ for **1** on the ac susceptibility. Data were taken at (△) 20, (●) 40 and (□) 240 Hz

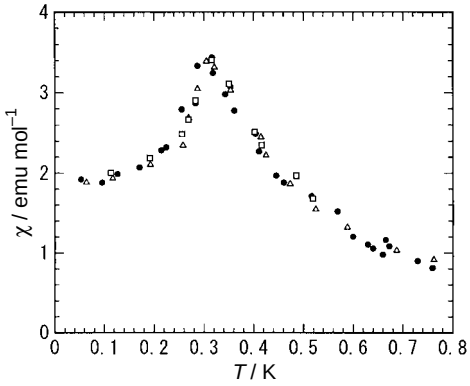


**Fig. 4** Temperature dependence of $\chi$ for **1** on the ac susceptibility in the low temperature region. Data were taken at (△) 20, (●) 40 and (□) 240 Hz

applied frequencies. In addition, no apparent hysteresis was observed between the cooling and heating cycles. Thus, ferromagnetic ordering with a $T_c$ of around 0.3 K is suggested to be responsible for the magnetic behavior of **1**.

An adiabatic heat capacity measurement was also performed on a powdered sample (547 mg) of radical **1**. A distinct peak was detected at the $T_c$ as shown in Fig. 5. The magnetic heat capacity of the paramagnetic state at higher temperatures is generally proportional to $T^{-2}$, while the lattice heat capacity is approximated by the Debye function with a $T^3$ dependence at low temperatures. A minimum, which can be seen at around 3 K in the inset of Fig. 5, corresponds to the overlapping of these two contributions with nearly the same magnitude. The magnetic heat capacity, $C_{mag}$, evaluated by subtracting the lattice contribution, shows the characteristic broad hump of a one-dimensional Heisenberg ferromagnet[10] and an intrachain exchange constant, $J/k_B$, of $0.6 \pm 0.1$ K. With the obtained values of $T_c$ and $J$, we can estimate the interchain interaction, $J'$, from mean field theory[11] or Oguchi's theory;[12] we find $J'/J$ to vary between 1/4 and 1/10. The overall heat capacity (Fig. 5 inset) is similar to that of the γ-phase *p*-NPNN with a quasi-one-dimensional magnetic structure.[10] We cannot determine the sign of $J'$ based on the present thermal analysis. However, considering the almost flat temperature dependence of the susceptibility below ≈0.25 K (Fig. 4), we presume $J' > 0$; if $J'$ is antiferromagnetic, the parallel susceptibility, which contributes one-third of the observed value for the powdered sample and decreases as the temperature decreases to zero, will also give the temperature dependence in this case.

In contrast to radical **1**, negative Weiss constants were obtained for radicals **2**, **3** and **4**, indicating that the intermo-

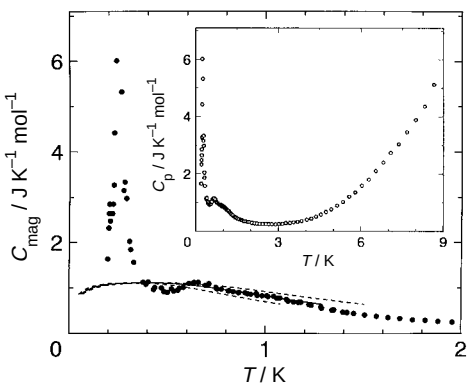


**Fig. 5** Temperature dependence of the magnetic heat capacity of **1** between 0.2 and 2 K. The solid line represents the theoretical results for an isotropic Heisenberg ferromagnet with $S = 1/2$ (one-dimensional Heisenberg ferromagnet) and $J/k_B = 0.6 \pm 0.1$ K. The data between 0.2 and 9 K is shown in the inset

lecular spin–spin interactions are antiferromagnetic in these three radicals; stronger interactions were observed in **3** and **4** than in the chlorine derivative **2** (Table 2). It is also notable that **3** and **4** show Weiss constants of almost the same order of magnitude, possibly reflecting the same degree of distortion (*cf.* Table 1).

Thus, a sharp difference was observed in the magnetic properties between **1** and the other derivatives and the origin of this difference could possibly be attributed, at least in part, to the degree of their molecular distortion, as estimated from the van der Waals radii of the halogen atom, and the resulting crystal structure differences in three dimensions.[13] In order to elucidate the magneto-structural correlation, we carried out an X-ray structural analysis on the fluorine derivative **1**, as well as on the chlorine derivative **2**.

## X-Ray Structural Analysis of 1 and 2

The molecular structure and atomic numbering of **1** are shown in Fig. 6.[14] The dihedral angle between the phenyl ring and the plane of the five-membered ring was found to be 48°, somewhat smaller than the value estimated from the MM calculations (Table 1). Molecular arrangements are shown in Fig. 7 (left, *a* axis projection) and in Fig. 8 (*b* axis projection). The

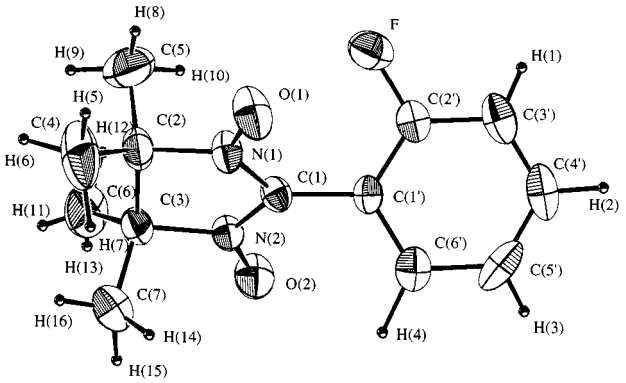


**Fig. 6** Molecular structure of **1**. Selected interatomic distances (Å) and angles (deg): O(1)—N(1) 1.26(1), N(1)—C(1) 1.34(1), C(1)—C(1′) 1.46(1), C(1′)—C(2′) 1.38(2), F—C(2′) 1.33(1); O(1)—N(1)—C(1) 126.3(8), N(1)—C(1)—C(1′) 125.9(8), C(1)—C(1′)—C(2′) 120.6(8), F—C(2′)—C(1′) 120.6(9)

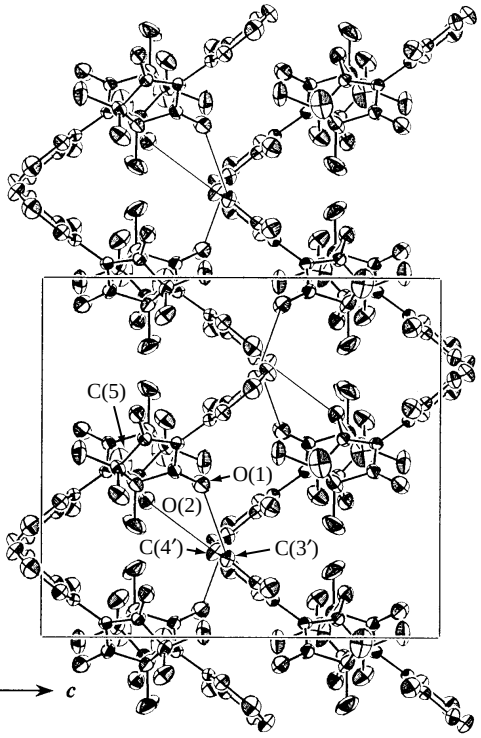


**Fig. 8** Crystal structure of **1** viewed along the *b* axis

structure consists of discrete elongated molecules approximately parallel to the *c* axis, which are symmetrically related by glide planes normal to the crystallographic axes and twofold screw axes parallel to them. Molecules are stacked in a head-to-tail and zigzag manner along the *a* axis and make up an infinite column (called the "a column" here). The nearest intermolecular NO—ON distance is 4.39 Å; this is thought to be too long for a direct interaction and hence, the overlapping of SOMOs between molecules is considered to be very small, which means that the magnetic interaction between them is very weak.[15] The intermolecular O—C lengths are relatively short and the three closest O—C pairs [O(1)—C(3′), O(2)—C(4′) and O(2)—C(5)] have distances of 3.229(8), 3.324(9) and 3.553(2) Å, respectively, which are depicted in Figs 7 and 8 as solid lines. These pairs link two

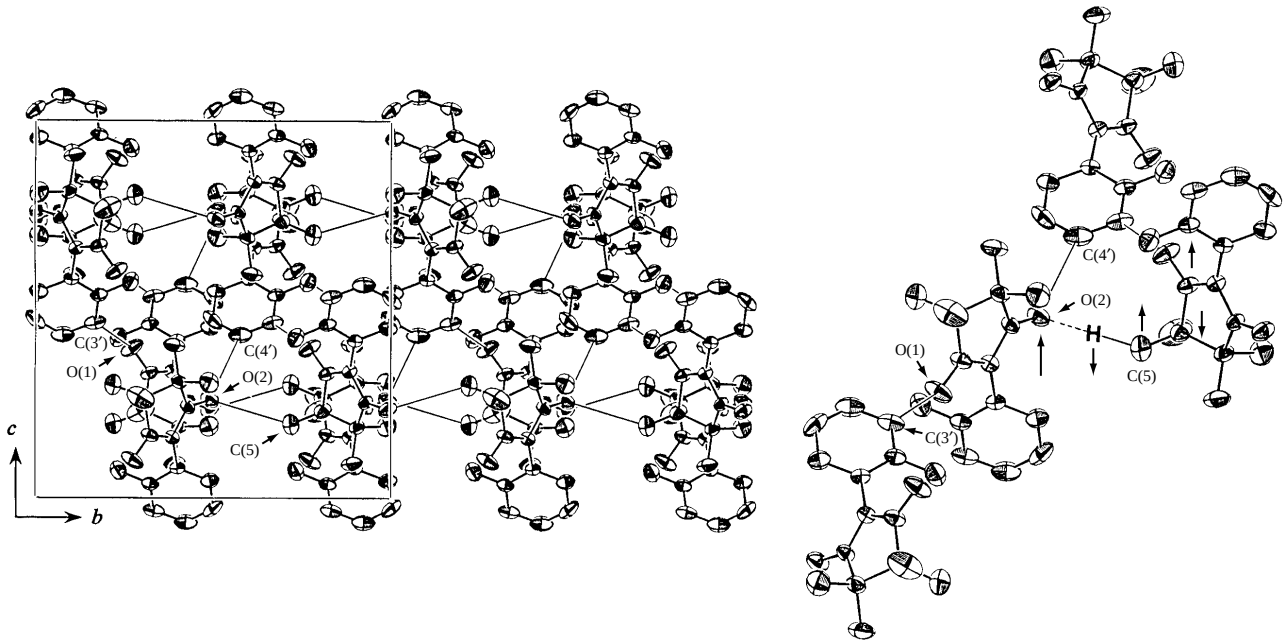


**Fig. 7** Left: crystal structure of **1** viewed along the *a* axis. Right: schematic figure to indicate possible spin polarization through O(2) and C(5)

neighboring molecules in neighboring columns to build up the three-dimensional network system *via* weak hydrogen bonds such as C—H···O—N (*cf.* Fig. 7, right)[16] or through other non-bonding interactions. Therefore, the spin–spin interactions between the radicals might work through methyl or phenyl groups to provide an efficient spin-polarization effect for the ferromagnetic interactions in them. While the quasi-one-dimensional feature of ferromagnetism in **1** would be due to the predominance of either of the spin–spin interactions described above, the observed ferromagnetic interactions are considered to be three-dimensional ones on the whole from the crystal structural analysis.

The molecular structure and atomic numbering of the chlorine derivative **2** are shown in Fig. 9. The dihedral angle between the phenyl ring and five-membered ring was found to be 60°, which is clearly a larger value than in **1**. Molecular arrangements are shown in Fig. 10 (left, *c* axis projection) and in Fig. 11 (*b* axis projection). The structure consists of discrete elongated molecules and they are symmetrically related by three two-fold screw axes parallel to the crystallographic axes. Molecules are stacked in a head-to-head and zigzag manner in the *ab* plane at *z* equal to 0 and 1/2 to make infinite layers. All molecules in one layer point in the same sense, nearly along

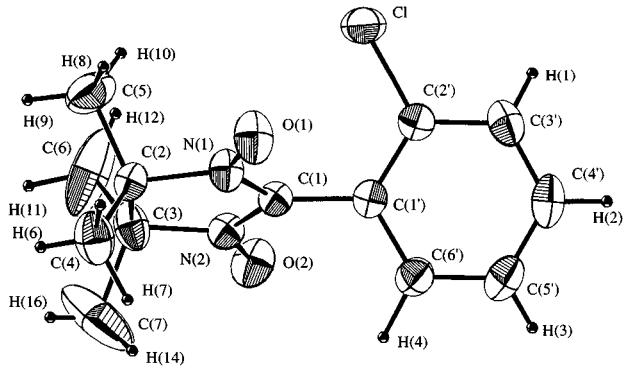


**Fig. 9** Molecular structure of **2**. Selected interatomic distances (Å) and angles (deg): O(1)—N(1) 1.274(2), N(1)—C(1) 1.341(3), C(1)—C(1′) 1.465(3), C(1′)—C(2′) 1.388(3), Cl—C(2′) 1.732(2); O(1)—N(1)—C(1) 126.0(2), N(1)—C(1)—C(1′) 124.6(2), C(1)—C(1′)—C(2′) 121.4(2), Cl—C(2′)—C(1′) 120.1(2)

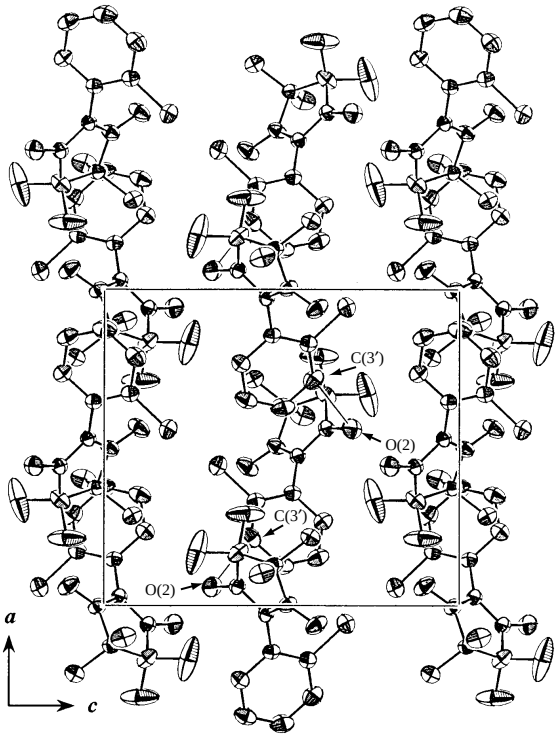


**Fig. 11** Crystal structure of **2** viewed along the *b* axis

the *a* axis, and those in the next layers point in the opposite sense. The nearest intermolecular O—C length is that of O(2)—C(3′) (3.34 Å), which are in the same layer and the spin–spin interactions between them are considered to be the main origin of the antiferromagnetic interactions observed in **2** (*cf.* Fig. 10, right)[17] because the nearest NO—ON distance is 5.40 Å, which is too long for direct spin–spin interactions. On the whole, the more severe twisting of the chlorine derivative **2** compared with the fluorine derivative **1** results in weaker three-dimensional interactions between the radicals and the spin polarization in the phenyl ring is considered to be less efficient, thus resulting in weak antiferromagnetic interactions between the spins in **2**.

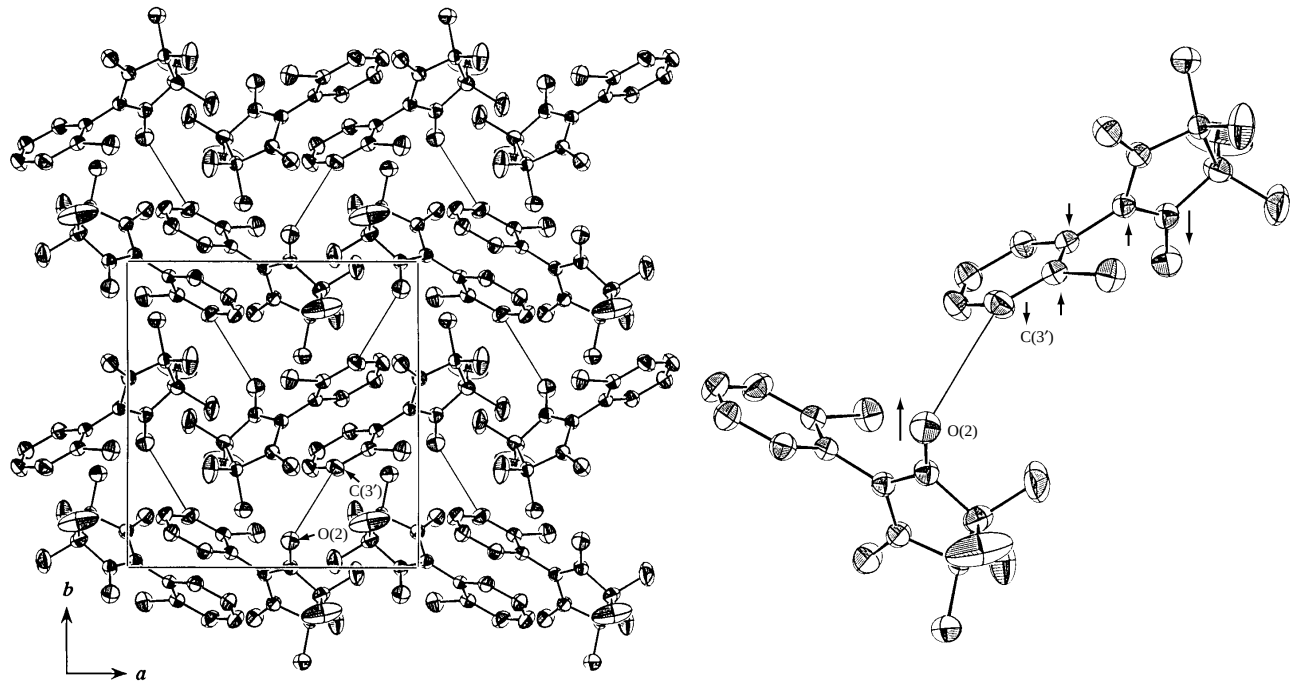


**Fig. 10** Left: crystal structure of **2** viewed along the *c* axis. Right: schematic figure to indicate possible spin polarization through O(2) and C(3′)

Antiferromagnetic behavior with a Weiss constant larger than that for **2** was found in the radicals **3** and **4**, whose molecular structures are possibly more distorted than **1** and **2**, based on theoretical analyses.

From the experimental results obtained in this study, it is recognized that the magnetic behavior of radical crystals depends upon their molecular structure and conformation, leading to different three-dimensional crystal structures and that, while a moderate degree of distortion can yield ferromagnetic interactions in the system, too much distortion (over 60°) results in antiferromagnetic interactions within the series investigated.

## Conclusions

We have prepared the nitronyl nitroxide derivatives of benzene bearing halogen atoms in the *ortho* position (**1**–**4**) to determine the effect of molecular distortion on their magnetic behavior. It was found from magnetic measurements that the fluorine derivative **1** showed ferromagnetic interactions while the other derivatives showed antiferromagnetic interactions; larger Weiss constants were found in the bromine **3** or iodine **4** derivatives than in the chlorine derivative **2**. The fluorine derivative **1** showed ferromagnetic behavior with a $T_c$ of around 0.3 K, elucidated by ac susceptibility and heat capacity measurements. Three-dimensional networks of the nitroxide radicals through the methyl and phenyl groups, demonstrated by the crystal structural analysis, were postulated to be at the origin of this magnetic behavior.

## Experimental

Melting points were measured on a Yamato MP-21 apparatus and are uncorrected. IR spectra were recorded on a Jasco Report-100 spectrometer. UV-visible spectra were obtained on Jasco Ubest-35 spectrometer. MS spectra were taken using a Jeol JMS-AX 505 mass spectrometer. ESR spectra were obtained on a Jeol JES-FE3XG spectrometer and each $g$ value was determined using $Mn^{2+}$/MnO as an internal standard. Susceptibility measurements were carried out on a Quantum Design MPMS-5 SQUID susceptometer using *ca.* 10 mg for each powdered sample at 0.5–1 T from 4.5 K to 300 K and 0.1 T below 4.5 K. The diamagnetic contributions were corrected using Pascal's constants. The ac susceptibility below 4.2 K was measured by a Hartshorn bridge circuit. The sample was connected to the mixing chamber of a 3He-4He dilution refrigerator and cooled down to about 40 mK. The earth magnetic field in the sample region was measured by a carbon thermometer and a CMN thermometer. All the reactions were carried out under nitrogen atmosphere. *o*-Halobenzaldehyde derivatives are commercially available except for *o*-iodobenzaldehyde and were used for the preparation of the corresponding free radicals. *o*-Iodobenzaldehyde was prepared by the oxidation of *o*-iodobenzyl alcohol with potassium dichromate and was used for further preparation.

### Syntheses of 2-(2′-halophenyl)-α-nitronyl nitroxide

**1**: To a stirred solution of *o*-fluorobenzaldehyde (0.15 g, 1.2 mmol) and 2,3-bis(hydroxyamino)-2,3-dimethylbutane sulfate (0.60 g, 2.4 mmol) in methanol (10 ml) was added anhydrous potassium carbonate (0.40 g, 2.9 mmol) at ambient temperature. Stirring was continued for a further 14.5 h and the resulting mixture was concentrated *in vacuo*. Benzene (15 ml) was added to the crude product, which was then filtered. To the filtrate was added lead(IV) oxide (1.0 g, 42 mmol); it was then stirred at ambient temperature for 1 h. The resulting mixture was filtered and washed with benzene to afford a deep violet solution, which after concentration was purified by column chromatography ($SiO_2$, 30 g) with benzene–ether as the eluent to give **1** as violet crystals (29 mg, 10% from the aldehyde). Single crystals were obtained by recrystallization from *n*-hexane. Mp. 125–126 °C. Anal. calcd (%) for $C_{13}H_{16}N_2O_2F$: C 62.14; H 6.42; N 11.15. Found C 62.53; H 6.55; N 11.40. UV/VIS: $\lambda_{max}$ ($CH_2Cl_2$)/nm (ε) 567 (600); EI-MS (70 eV): $m/z$ 251 $[M]^+$; ESR (benzene): $g = 2.007$, $a_N = 0.70$ mT.

In a similar manner, the other derivatives (**2**, **3**, **4**) were prepared.

**2**: Dark violet crystals. Mp. 121–122 °C. Anal. calcd (%) for $C_{13}H_{16}N_2O_2Cl$: C 58.32; H 6.02; N 10.47. Found C 58.67, H 6.43, N 10.27. UV/VIS: $\lambda_{max}$ ($CH_2Cl_2$)/nm (ε) 551 (700); EI-MS (70 eV): $m/z$ 267 $[M]^+$, 269 $[M + 2]^+$; ESR (benzene): $g = 2.008$, $a_N = 0.73$ mT.

**3**: Dark violet crystals. Mp. 130–131 °C. Anal. calcd (%) for $C_{13}H_{16}N_2O_2Br$: C 50.02; H 5.17; N 8.98. Found C 50.48; H 5.16; N 9.00. UV/VIS: $\lambda_{max}$ ($CH_2Cl_2$)/nm (ε) 547 (600); EI-MS (70 eV): $m/z$ 311 $[M]^+$, 313 $[M + 2]^+$; ESR (benzene): $g = 2.008$, $a_N = 0.71$ mT.

**4**: Dark violet crystals. Mp. 163 °C. Anal. calcd (%) for $C_{13}H_{16}N_2O_2I$: C 43.47; H 4.49; N 7.80. Found C 43.63; H 4.43; N 7.43. UV/VIS: $\lambda_{max}$ ($CH_2Cl_2$)/nm (ε) 548 (800); EI-MS (70 eV): $m/z$ 359 $[M]^+$; ESR (benzene): $g = 2.008$, $a_N = 0.71$ mT.


## Acknowledgements

We are grateful to Profs. Masaaki Ohmasa and Hajime Saito of the Himeji Institute of Technology for their kind advice. This research was supported by a Grant-in-Aid for Scientific Research on Priority Area "Molecular Magnetism" (No. 228/04242104) from the Ministry of Education, Science and Culture, Japan and a Scientific Research Grant from The Foundation of Himeji Institute of Technology, which are gratefully acknowledged.


## References


1 Part of this work has been presented at The Vth International Conference on Molecular-Based Magnets held in Osaka, July 1996; S. Nakatsuji, M. Saiga, N. Itaga, M. Nakagawa, Y. Oda, K. Suzuki, T. Enoki and H. Anzai, *Mol. Cryst. Liq. Cryst.*, 1997, **306**, 279.

2 *Cf.* H. Iwamura, *Adv. Phys. Org. Chem.*, 1990, **26**, 179; O. Kahn, *Molecular Magnetism*, VCH, Weinheim, 1993; J. S. Miller and A. J. Epstein, *Angew. Chem., Int. Ed. Engl.*, 1994, **33**, 385.

3 M. Kinoshita, P. Turek, M. Tamura, K. Nozawa, D. Shiomi, Y. Nakazawa, M. Ishikawa, M. Takahashi, K. Awaga, T. Inabe and Y. Maruyama, *Chem. Lett.*, 1991, 1225.

4 R. Chiarelli, M. A. Novak, A. Rassat and J. L. Tholence, *Nature (London)*, 1993, **363**, 147; T. Nogami, K. Tomioka, T. Ishida, H. Yoshikawa, M. Yasui, F. Iwasaki, H. Iwamura, N. Takeda and M. Ishikawa, *Chem. Lett.*, 1994, 29; T. Ishida, H. Tsuboi, T. Nogami, H. Yoshikawa, M. Yasui, F. Iwasaki, H. Iwamura, N. Takeda and M. Ishikawa, *Chem. Lett.*, 1994, 919; T. Mukai, K. Konishi, K. Nedachi and K. Takeda, *J. Magn. Magn. Mater.*, 1995, **140–144**, 1449.

5 β-phase: K. Awaga, T. Inabe, U. Nagashima and Y. Maruyama, *J. Chem. Soc., Chem. Commun.*, 1989, 1617. A 2D network through the weak intermolecular contacts between the O atoms in the NO groups and the N atoms in the $NO_2$ groups are reported to be responsible in this conformation. γ-phase: P. Turek, K. Nozawa, D. Shiomi, K. Awaga, T. Inabe, Y. Maruyama and M. Kinoshita, *Chem. Phys. Lett.*, 1991, **180**, 327.

6 T. Sugawara, M. M. Matsushita, A. Izuoka, N. Wada, N. Takeda and M. Ishikawa, *J. Chem. Soc., Chem. Commun.*, 1994, 1723.

7 J. Cirujeda, M. Mas, E. Molins, F. L. de Panthou, J. Laaugier, J. G. Park, C. Paulsen, P. Rey, C. Rovira and J. Veciana, *J. Chem. Soc., Chem. Commun.*, 1995, 709.

8 The magnetic properties and crystal structure of *p*-fluorophenyl nitronyl nitroxide have recently been reported: Y. Hosokoshi, M. Tamura, M. Kinoshita, H. Sawa, Y. Fujiwara and Y. Ueda, *J. Mater. Chem.*, 1994, **4**, 1219.

9 E. F. Ullman, J. H. Osiecki, D. G. B. Boocock and R. Darcy, *J. Am. Chem. Soc.*, 1972, **94**, 7049.
10 Y. Nakazawa, M. Tamura, N. Shirakawa, D. Shiomi, M. Takahashi, M. Kinoshita and M. Ishikawa, *Phys. Rev. B*, 1992, **46**, 8906.
11 M. Steiner, J. Villain and C. G. Windsor, *Adv. Phys.*, 1976, **25**, 199.
12 T. Oguchi, *Phys. Rev.*, 1964, **133A**, 1098.
13 Besides the steric effect, the electronic effects of halogen atoms could also be considered to contribute in part to the difference, especially in the construction of three-dimensional crystal structures. Considerable attention has been focused in recent years on using weak intermolecular interactions to construct supramolecular structures in crystal engineering; *cf.* G. R. Desiraju, *Angew. Chem., Int. Ed. Engl.*, 1995, **34**, 2311 and references cited therein.
14 Crystal data for **1**: $C_{13}H_{16}N_2O_2F$, $M = 251.29$, orthorhombic, space group *Pbca*, $a = 13.180(3)$, $b = 13.764(6)$, $c = 14.438(4)$ Å. $T = 24 \pm 1$ °C. $V = 2619.2(14)$ Å$^3$, $Z = 8$, $D_c = 1.280$ g cm$^{-3}$. $F(000) = 1072$. 6350 measured reflections, 6350 unique reflections, collected on a Enraf-Nonius four-circle diffractometer with monochromatic MoKα radiation (0.710 73 Å). Final conventional *R* factor 0.092, weighed *R* factor 0.076 for 1317 independent reflections with $F_0 > 3\sigma(F_0)$ and 227 parameters. Crystal data for **2**: $C_{13}H_{16}N_2O_2Cl$, $M = 267.74$, orthorhombic, space group $P2_12_12_1$, $a = 10.496(3)$, $b = 10.933(4)$, $c = 11.681(5)$ Å. $T = 24 \pm 1$ °C. $V = 1340.4(8)$ Å$^3$, $Z = 4$, $D_c = 1.327$ g cm$^{-3}$. $F(000) = 564$. 3304 unique reflections collected on a Enraf-Nonius CAD4 computer-controlled kappa axis diffractometer with monochromatic MoKα radiation (0.710 73 Å). Final *R* factor 0.044, weighed *R* factor 0.035 for 2546 independent reflections with $F_0 > 1.5\ \sigma(F_0)$ and 227 variable parameters. CCDC reference number 440/017.
15 K. Awaga and Y. Maruyama, *J. Chem. Phys.*, 1989, **91**, 2743.
16 T. Nogami, T. Ishida, H. Tsuboi, H. Yoshikawa, H. Yamamoto, M. Yasui, F. Iwasaki, H. Iwamura, N. Takeda and M. Ishikawa, *Chem. Lett.*, 1995, 635; J. Veciana, J. Cirujeda, C. Rovira and J. Vidal-Gancedo, *Adv. Mater.*, 1995, **7**, 221.
17 *Cf.* H. M. McConnell, *J. Chem. Phys.*, 1963, **39**, 1910; for a recent review, see C. Kollar and O. Kahn, *Acc. Chem. Res.*, 1993, **26**, 259.

*Received* 21*st October* 1996; *revised M/S received* 9*th June* 1997; *Paper* 7/08328I